

# Stable many-body resonances in open quantum systems

Ruben Peña,<sup>1</sup> Thi Ha Kyaw,<sup>2</sup> and Guillermo Romero<sup>1,3,\*</sup>

<sup>1</sup>*Departamento de Física, Universidad de Santiago de Chile, Avenida Víctor Jara 3493, 9170124, Santiago, Chile*

<sup>2</sup>*LG Electronics Toronto AI Lab, Toronto, Ontario M5V 1M3, Canada*

<sup>3</sup>*Center for the Development of Nanoscience and Nanotechnology, Estación Central, 9170124, Santiago, Chile*

(Dated: September 16, 2022)

Periodically driven quantum many-body systems exhibit novel nonequilibrium states such as prethermalization, discrete time crystals, and many-body localization. Recently, it has been proposed the general mechanism of fractional resonances that leads to the slowing of the many-body dynamics in systems with both  $U(1)$  and parity symmetry. Here, we show that fractional resonance is a stable phenomenon under local noise models. To corroborate our finding, we numerically study the dynamics of the Bose-Hubbard model, small scale of which can readily be implemented in existing noisy intermediate-scale quantum (NISQ) devices. Our findings suggest a possible pathway towards stable nonequilibrium state-of-matter, with potential applications of quantum memories for quantum information processing.

## I. INTRODUCTION

Nonequilibrium quantum phases without static analogs have become an active area of research since programmable quantum simulators [1] such as cold atoms [2–5] and superconducting circuits [6–11] allow the preparation of exotic states of matter into out-of-equilibrium. Paradigmatic examples of nonequilibrium states are discrete time crystals [12–21] and Floquet prethermalization [22–29]. The search for nonequilibrium states of matter is challenging since one needs to move beyond standard quantum statistical mechanics [30–34] and simulations of quantum many-body systems in classical computers [35–37]. In a recent contribution by some of the authors [38], it has been pointed out that emergence of a prethermal and localized nonequilibrium phase, termed “fractional resonance”, appearing in a broad class of many-body Hamiltonians exhibiting  $U(1)$  and parity symmetry such as the Bose-Hubbard model [39, 40], the XXZ spin-1 model [41, 42] or the Jaynes-Cummings-Hubbard model [43–45]. Moreover, small-scale versions of these models can be experimentally implemented in NISQ devices. Therefore, we believe it is pertinent to ask for the stability of such nonequilibrium states of matter under the action of loss mechanisms, which will be relevant for applications in quantum memories [46] and quantum metrology [47].

On the other hand, quantum computing [48] and quantum machine learning [49–51] are progressing tremendously. The main driving force behind this progress is that quantum computers promise exponential speedup over their classical counterparts in solving specific tasks [52]. When fault-tolerant general-purpose quantum computers become available in the long term, it is expected to implement adiabatic state preparation and quantum phase estimation as the standard quantum routine to determine the ground state energy of a sophisticated physical Hamiltonian [53–56]. However, such schemes are resource intensive, and thus they are not appropriate for current NISQ hardware [57–61], thereby shifting the central research theme towards low-depth hybrid quantum-classical algorithms, otherwise known as NISQ algorithms [62]. Recently, by utilizing quantum data processing, learning certain

information about a many-body quantum state from an experiment can be exponentially reduced [63–65]. In contrast, in the standard classical paradigm, one must repeat the experiment many times to build statistical certainty about the measurement data at each experimental run. By loading the entire quantum state of a many-body system into a quantum memory, a shift in the paradigm occurs in a new approach. After some quantum processing is applied to the replicated state, measurements are performed. Then the protocol can be repeated. Furthermore, renowned quantum machine learning algorithms center around the Harrow-Hassidim-Lloyd (HHL) algorithm [66] and quantum principal component analysis [67], which require the physical realization of quantum random access memory [68, 69]. Here we recognize a substantial overlap with localized nonequilibrium states of matter, such as prethermal states [22–29] and many-body localization [70–72]. Moreover, because localized nonequilibrium states of matter retain information about their initial state, they have the potential to be used as quantum memories [73]. These and the above arguments indicate that developing and realizing a quantum memory represents the pinnacle achievement in quantum technologies and applications.

In this article, we provide a detailed analysis of the stability of fractional many-body resonances under noisy environments within the paradigm of NISQ devices. This investigation represents an important step before seeking potential applications of fractional resonances and their associated prethermal states as a quantum memory. The article is organized as follows. In section II, we briefly recap the emergence of many-body resonances, emphasizing the integer and fractional resonance states, with the use of a generic Hamiltonian. In section III, we consider a one-dimensional lattice of strongly correlated bosonic particles described by the Bose-Hubbard model (BHM) [39, 40], where we study the open quantum system dynamics of the BHM, and discuss the stability of integer and fractional resonance states when considering realistic parameters of NISQ devices such as superconducting circuits, for the sake of simulating the prescribed physics in an experiment. Finally, in section IV, we present our concluding remarks.

\* [guillermo.romero@usach.cl](mailto:guillermo.romero@usach.cl)

## II. THE MODEL

Let us consider a one-dimensional lattice with open boundary conditions described by the generic lattice Hamiltonian

$$\hat{H} = \hbar \sum_{j=1}^L (\omega \hat{O}_j + \frac{U}{2} \hat{O}_j^2) - \hbar J_0 \cos(\Omega t) \sum_{j=1}^{L-1} (\hat{A}_j^\dagger \hat{A}_{j+1} + \hat{A}_{j+1}^\dagger \hat{A}_j), \quad (1)$$

which is composed of a local energy term  $\hat{H}_0 \equiv \hbar \sum_{j=1}^L (\omega \hat{O}_j + U \hat{O}_j^2/2)$  with local operators  $\hat{O}_j$ , and a time-dependent hopping interaction  $\hat{H}_I(t) = \hbar J_0 \cos(\Omega t) \sum_{j=1}^{L-1} (\hat{A}_j^\dagger \hat{A}_{j+1} + \hat{A}_{j+1}^\dagger \hat{A}_j)$ , allowing for the exchange of particles/exitations between the nearest neighboring sites via the local ladder operators  $\hat{A}_j$  and  $\hat{A}_j^\dagger$ . These operators satisfy the commutation relations  $[\hat{O}_i, \hat{A}_j^\dagger] = \delta_{ij} \hat{A}_j^\dagger$ ,  $[\hat{O}_i, \hat{A}_j] = -\delta_{ij} \hat{A}_j$ . Here, we restrict ourselves in studying bosonic particles. However, the treatment is also applicable to spin- $d$  systems. If the many-body system is isolated from an external environment, the term  $\sum_{j=1}^N \omega \hat{O}_j$  is a constant of motion since the Hamiltonian exhibits U(1) symmetry. The Hermitian operator  $\hat{O}_j$  satisfies the eigenvalue equation  $\hat{O}_j |m_j\rangle = m_j |m_j\rangle$ , where  $m_j$  is a quantum number that labels the local quantum state of the  $j$ th lattice site. For instance,  $m_j$  may represent the occupation number of a bosonic system or the spin component along the  $z$  direction of spin- $d$  systems. In this work, we focus on finite-size lattices with reflection symmetry characterized by the parity operator  $\hat{P}$ , which satisfies  $\hat{P} |m_1, \dots, m_j, \dots, m_L\rangle = |m_L, \dots, m_j, \dots, m_1\rangle$ , where  $|m_1, \dots, m_j, \dots, m_L\rangle \equiv \bigotimes_{l=1}^L |m_l\rangle$ .

To understand the processes that may occur due to the hopping of particles/exitations, let us move to a rotating frame

with respect to the free Hamiltonian  $\hat{H}_0$ . We obtain

$$\begin{aligned} \tilde{H}_I(t) = & -\hbar J_0 \cos(\Omega t) \sum_{j=1}^{L-1} \left[ e^{iUt(\hat{O}_{j+1} - \hat{O}_{j-1})} \hat{A}_j^\dagger \hat{A}_{j+1} \right. \\ & \left. + \hat{A}_{j+1}^\dagger \hat{A}_j e^{-iUt(\hat{O}_{j+1} - \hat{O}_{j-1})} \right], \end{aligned} \quad (2)$$

from which we can identify two characteristic time scales: one is provided by the driving frequency  $\Omega$ , and another is the on-site interaction  $U$ , which leads to a local anharmonic spectrum. The Hamiltonian (2) is not strictly periodic neither in  $\Omega$  nor  $U$ . However, we will consider integer and fractional driving frequencies in the unit of  $U$  defined as  $\Omega = U$  and  $\Omega = U/2$ , respectively. In both cases, it can be shown that  $\tilde{H}_I(t+T) = \tilde{H}_I(t)$  is periodic with period  $T = 2\pi/\Omega$  [38]. Also, we consider the strongly interacting regime where  $U \gg J_0$  [3], where  $J_0$  is the bare (static) hopping rate. This regime allows us to describe the particle/excitation hopping processes within the semi-classical picture as discussed in the Refs. [29, 38].

Let us briefly describe the aforementioned semi-classical picture to identify many-body resonances [74] in the closed system scenario. To find many-body resonances we focus on how specific quantum states, referred to as configurations, are connected via the hopping term. Let us suppose the many-body system is initialized in the configuration  $|m_1, \dots, m_j, m_k, m_l, \dots, m_L\rangle$ , a hopping event from site  $j$  to  $k$  will lead the system to occupy the state  $|m_1, \dots, m_j - 1, m_k + 1, m_l, \dots, m_L\rangle$ . Now, let us compute the local energy of those states using the unperturbed Hamiltonian  $\hat{H}_0$ . The result reads

$$\hat{H}_0 |m_1, \dots, m_j, m_k, m_l, \dots, m_L\rangle = \hbar \sum_{j=1}^L \left( \omega m_j + \frac{U}{2} m_j^2 \right) |m_1, \dots, m_j, m_k, m_l, \dots, m_L\rangle \quad (3a)$$

$$\hat{H}_0 |m_1, \dots, m_j - 1, m_k + 1, m_l, \dots, m_L\rangle = \hbar \left[ \sum_{j=1}^L \left( \omega m_j + \frac{U}{2} m_j^2 \right) + U(m_k - m_j + 1) \right] |m_1, \dots, m_j - 1, m_k + 1, m_l, \dots, m_L\rangle. \quad (3b)$$

The energy difference between these two configuration is  $\Delta E = \hbar U(m_k - m_j + 1)$ . Therefore, to evolve from the state  $|m_1, \dots, m_j, m_k, m_l, \dots, m_L\rangle$  to  $|m_1, \dots, m_j - 1, m_k + 1, m_l, \dots, m_L\rangle$ , the driving frequency should match the condition  $m\Omega = U(m_k - m_j + 1)$ . Analogously, it can be shown that a hopping event from  $k \rightarrow j$  leads to the condition  $m\Omega = U(m_j - m_k + 1)$ , so we can write generically  $m\Omega = U[\pm(m_k - m_j) + 1]$ , with  $m \in \mathbb{Z}$ , which defines the integer many-body resonance [29, 38]. In this case, the emerging many-body dynamics is ruled by nearest-neighbor interactions where the time scale for the spreading of particles/exitations is  $J_0^{-1}$ .

In a recent work, it has been proposed the emergence of fractional resonances in many-body quantum systems where second-order processes rule the nonequilibrium dynamics [38]. In this article, we have rigorously demonstrated the emergence of fractional resonance condition using the Magnus expansion [75–77]. Here, we will follow the semi-classical picture described above to find the fractional resonance condition.

If the initial configuration is  $|m_1, \dots, m_j, m_k, m_l, \dots, m_L\rangle$ , we want to connect this state with  $|m_1, \dots, m_j - 1, m_k, m_l + 1, \dots, m_L\rangle$  via two hopping events. Notice that the latter configuration has local energy  $\hbar \sum_{j=1}^L \left( \omega m_j + \frac{U}{2} m_j^2 \right) + \hbar U(m_l - m_j + 1)$ . The energy

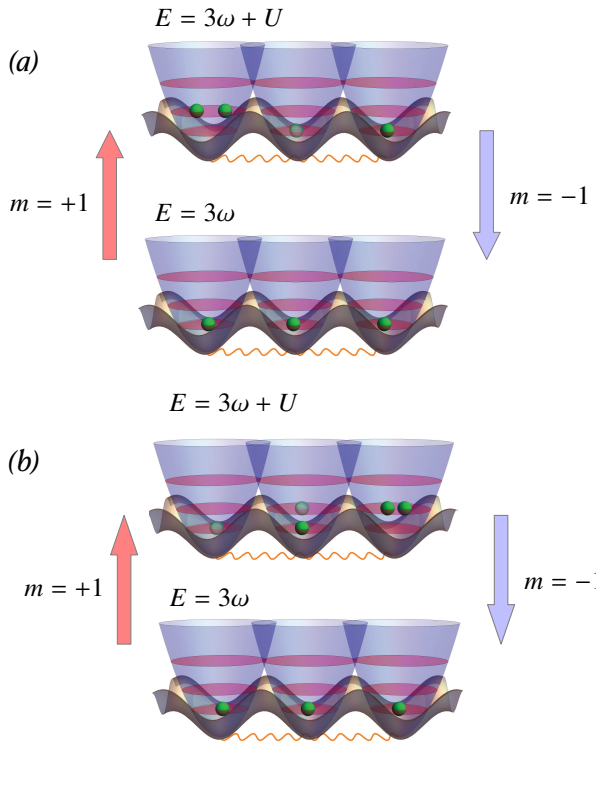


Figure 1. Schematic representation of many-body resonances in the driven lattice model. a) The panel shows a transition from the initial condition  $m_j = m_k = m_l = 1$  with particles (green circles) occupying each lattice site (from bottom to top). Here, we represent a hopping event where the middle particle moves to the left-most site, reaching the configuration  $m_j = 2, m_k = 0, m_l = 1$ . The energy difference between these configurations is  $\Delta E = \hbar U$ . b) The panel shows a transition from the initial condition  $m_j = m_k = m_l = 1$  with particles (green circles) occupying each lattice site (from bottom to top). The top panel shows two hopping events where the left-most particle moves to the right-most site, reaching the configuration  $m_j = 0, m_k = 1, m_l = 2$ . The energy difference between these configurations is also  $\Delta E = \hbar U$ . Therefore, within the semi-classical picture, each hopping event increases the system energy by a factor of  $\hbar U/2$ .

difference between this configuration and the initial one is  $\Delta E = \hbar U(m_l - m_j + 1)$ . Therefore, in order to connect both configurations, it is necessary two identical hopping events each kicking the system with energy  $\hbar U(m_l - m_j + 1)/2$ . The same analysis can be done for a hopping from  $j \rightarrow l$  leading to the condition  $\Omega = U(m_j - m_l + 1)/2$ , so we can write generically  $m\Omega = U[\pm(m_j - m_l) + 1]/2$ , where  $m \in \mathbb{Z}$ .

In order to better illustrate integer and fractional resonance conditions, let us consider the schematic representation of figure 1. Here, we display a schematic representation of many-body resonances in the driven lattice model. In figure 1(a), we show two configurations with all particles (green circles) occupying a lattice site and the left-most site occupied by two particles. The energy difference between these configurations is  $\Delta E = \hbar U$ . Therefore, to evolve from the lower to the upper configuration, one needs to activate a hopping event with

frequency  $\Omega = U$  to increase the system energy. In figure 1(b), we show configurations that involve two hopping events where the left-most particle moves to the right-most lattice site. The energy difference between these configurations is  $\Delta E = \hbar U$ , so that each hopping event increases the system energy by a factor of  $\hbar U/2$ .

Along this work we will prove that the emergent many-body fractional resonance is a stable phenomenon under loss mechanisms inherent to NISQ devices. In particular, we will numerically study the nonequilibrium dynamics of the Bose-Hubbard model [40, 78, 79], which allows us to describe implementations of strongly interacting lattice systems in superconducting circuits [6–8, 10, 80–82].

### A. The Bose-Hubbard Model

The Bose-Hubbard model (BHM) describes strongly interacting bosonic systems on a lattice, where we recognize operators  $\hat{O}_j = \hat{n}_j = \hat{a}_j^\dagger \hat{a}_j$ ,  $\hat{a}_j^\dagger = \hat{A}_j^\dagger$ , and  $\hat{a}_j = \hat{A}_j$ . Replacing these operator in the generic Hamiltonian (1) we can generate the Bose-Hubbard Hamiltonian

$$\hat{H}(t) = \hbar \sum_{j=1}^L (\omega \hat{n}_j + \frac{U}{2} \hat{n}_j^2) - \hbar J(t) \sum_{j=1}^{L-1} (\hat{a}_j^\dagger \hat{a}_{j+1} + \hat{a}_{j+1}^\dagger \hat{a}_j), \quad (4)$$

where  $\hat{a}_j(\hat{a}_j^\dagger)$  is the annihilation (creation) bosonic operator at site  $j$ ,  $\omega$  is the single site frequency,  $U$  the on-site interaction,  $J(t) = J_0 \cos(\Omega t)$  the modulated hopping strength between neighboring sites, whereas  $J_0$  is the bare hopping rate, and  $\Omega$  the driving frequency. We stress that modulating the hopping rate can be achieved in superconducting circuits with transmons [11]. The symmetries of the Hamiltonian (4) play a crucial role for describing the many-body dynamics. In particular, the BHM exhibits  $U(1)$  symmetry characterized by the conservation of the total number of particles/exitations  $[\hat{H}, \hat{N}] = 0$  with  $\hat{N} = \sum_{j=1}^L \hat{a}_j^\dagger \hat{a}_j$ . Also, since we consider a lattice with open boundary conditions, the model preserves the parity  $[\hat{H}, \hat{P}]$ , where  $\hat{P}|n_1, n_2, \dots, n_L\rangle = |n_L, \dots, n_2, n_1\rangle$ , where  $n_j$  stands for the number of particles/exitations at the  $j$ th lattice site. Hereafter, we will consider a initial with unit filling, that is,  $|\psi_0\rangle = \bigotimes_{j=1}^L |1\rangle_j$ . In general, the total number of states that may be involved in the dynamics correspond to all possible configurations of  $N$  particles distributed in  $L$  lattice sites  $D_{N,L} = (N + L - 1)!/N!(L - 1)!$ .

### III. OPEN QUANTUM SYSTEM DYNAMICS

Realistic implementations of a strongly correlated bosonic systems in superconducting circuits always involve the interaction with some electromagnetic environment which leads to a noisy dynamics. NISQ devices made of superconducting circuits have proven successful to stabilize nonequilibrium many-body states [6–11, 28], whose features are well captured by the BHM [39, 40]. In these experiments, the open system

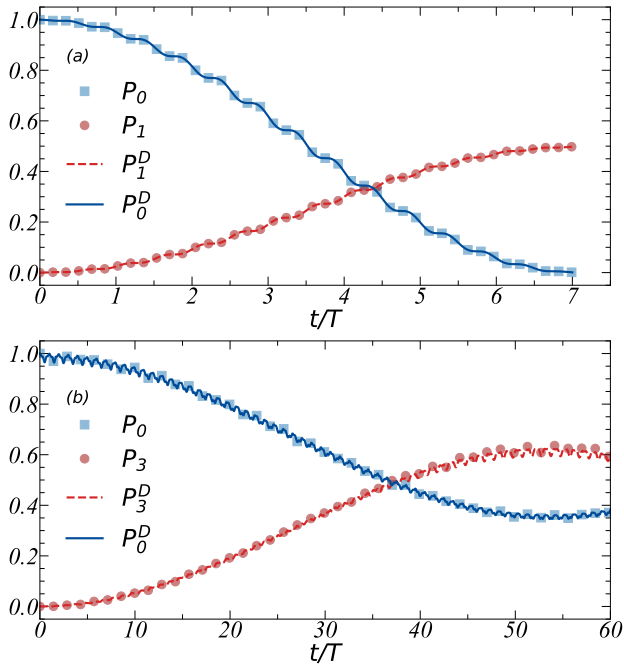


Figure 2. The upper panel (a) shows the populations of states  $|\psi_i\rangle$  with  $i = 0, 1$  for the integer resonance  $\Omega = U$ . The lower panel (b) shows the populations of states  $|\psi_i\rangle$  with  $i = 0, 3$  for the fractional resonance  $\Omega = U/2$ . In both panels,  $P_i^D$  with  $i = 0, 1, 3$  are populations numerically obtained considering decay and dephasing for each lattice site, whereas  $P_i$  with  $i = 0, 1, 3$  are populations numerically computed considering a closed system scenario. Also, the three-site Bose-Hubbard lattice is initialized in the state  $|\psi_0\rangle = |111\rangle$  and we use realistic parameters  $\omega = 2\pi \times 4.5$  GHz,  $J = 2\pi \times 11.5$  KHz,  $\kappa_{10} = 11.9$  KHz,  $\kappa_{21} = 24.39$  KHz,  $\kappa_{32} = 33.33$  KHz,  $\gamma_{01} = 13.89$  KHz,  $\gamma_{12} = 31.25$  KHz,  $\gamma_{23} = 83.33$  KHz.

dynamics is well described by the Lindblad master equation

$$\frac{d\hat{\rho}}{dt} = -\frac{i}{\hbar} [\hat{H}(t), \hat{\rho}(t)] + \sum_{j=1}^L \sum_{l=a,n} \frac{1}{2} [2\hat{C}_{l,j}\hat{\rho}(t)\hat{C}_{l,j}^\dagger - \hat{\rho}(t)\hat{C}_{l,j}^\dagger\hat{C}_{l,j} - \hat{C}_{l,j}^\dagger\hat{C}_{l,j}\hat{\rho}(t)], \quad (5)$$

where  $l$  and  $j$  label different types of loss mechanisms and  $j$ th lattice site, respectively. In this work, we consider decay ( $l = a$ ) and dephasing ( $l = n$ ) acting upon each bosonic particle. Also, we consider finite lattices with  $L = 3$  and  $L = 4$  sites with up to  $n_{\max} = 3$  particles per site with local Hilbert space dimension  $\dim(\mathcal{H}_l) = 4$ . In this case, a multi-level approach with states  $\{|0\rangle, |1\rangle, |2\rangle, |3\rangle\}$  playing the key role in the emerging many-body dynamics must be included in the Lindblad master equation (5) as follows. We define collapse operators at the  $j$ th site as

$$C_{a,j} = \begin{pmatrix} 0 & \sqrt{\kappa_{10}} & 0 & 0 \\ 0 & 0 & \sqrt{2\kappa_{21}} & 0 \\ 0 & 0 & 0 & \sqrt{3\kappa_{32}} \\ 0 & 0 & 0 & 0 \end{pmatrix} \quad (6a)$$

$$C_{n,j} = \begin{pmatrix} 0 & 0 & 0 & 0 \\ 0 & \sqrt{\gamma_{01}} & 0 & 0 \\ 0 & 0 & 2\sqrt{\gamma_{12}} & 0 \\ 0 & 0 & 0 & 3\sqrt{\gamma_{23}} \end{pmatrix}, \quad (6b)$$

where  $\kappa_{rs}$  and  $\gamma_{rs}$  define decay and dephasing rates, respectively. In the decay rates, the subindexes  $r, s$  refer to the decay from the state  $|r\rangle$  to  $|s\rangle$ , whereas in the dephasing rates refer to the dephasing for the superpositions of states  $|r\rangle$  and  $|s\rangle$ , within each lattice site  $j$ .

### A. The three-site Bose-Hubbard lattice

Let us consider a three-site Bose-Hubbard lattice. We will present results about the stability of the emerging many-body dynamics when considering fractional ( $\Omega = U/2$ ) and integer ( $\Omega = U$ ) resonance conditions in an open system scenario. Our study involves the numerical solution of the Lindblad master equation (5) using the fourth order Runge-Kutta algorithm. As initial condition we consider a product state with unit filling  $|\psi_0\rangle = |111\rangle$ . In a closed system scenario, the system will only populate states within the positive parity subspace  $|\psi_0\rangle$ ,  $|\psi_1\rangle = \frac{1}{\sqrt{2}}(|120\rangle + |021\rangle)$ ,  $|\psi_2\rangle = \frac{1}{\sqrt{2}}(|102\rangle + |201\rangle)$ ,  $|\psi_3\rangle = \frac{1}{\sqrt{2}}(|210\rangle + |012\rangle)$ ,  $|\psi_4\rangle = |030\rangle$ ,  $|\psi_5\rangle = \frac{1}{\sqrt{2}}(|300\rangle + |003\rangle)$  [38]. In an open system scenario, we expect that U(1) symmetry will no longer be preserved. In our model, we will consider identical loss mechanisms for each lattice sites that implies parity symmetry is still preserved. In this article, we demonstrate that many-body resonances and their emerging dynamical features are stable phenomena under loss mechanisms inherent to NISQ devices.

In figure 2(a) we plot the populations of states  $|\psi_i\rangle$  with  $i = 0, 1$  for the integer resonance condition  $\Omega = U$ . The lower panel (b) shows the populations of states  $|\psi_i\rangle$  with  $i = 0, 3$  for the fractional resonance condition  $\Omega = U/2$ . We identify populations as  $P_i(t) = |\langle\psi_i|\psi(t)\rangle|^2$ . In both panels,  $P_i$  with  $i = 0, 1, 3$  are populations numerically computed considering a closed system scenario governed by the Hamiltonian (4), and  $P_i^D$  with  $i = 0, 1, 3$  are populations numerically obtained considering decay and dephasing mechanisms acting upon each lattice site. We stress that the populations of states  $|\psi_1\rangle$  and  $|\psi_2\rangle$  are the same, so we only show  $P_1(t)$  along this work.

In our numerical simulations we use realistic values for decay ( $\kappa_{jk}$ ) and dephasing ( $\gamma_{jk}$ ) rates of superconducting circuit experiments [83]. Also, single site frequency  $\omega$  and hopping rate  $J_0$  are taken from Ref.[10], and  $U = 40J_0$ , see the caption of figure 2 for details. The results shown in figure 2 allow us to conclude that noisy mechanisms negligibly affect the emerging dynamics of many-body resonances. It is worth mentioning that despite the long time needed for the population of state  $|\psi_3\rangle$  to occur with highest probability in the fractional resonance case, the system dynamics is robust under loss mechanisms.

When considering a noisy dynamics, the U(1) symmetry is broken and the system could populate states outside the unit filling subspace. In this case, the wave function may be written as a linear combination of all possible configurations

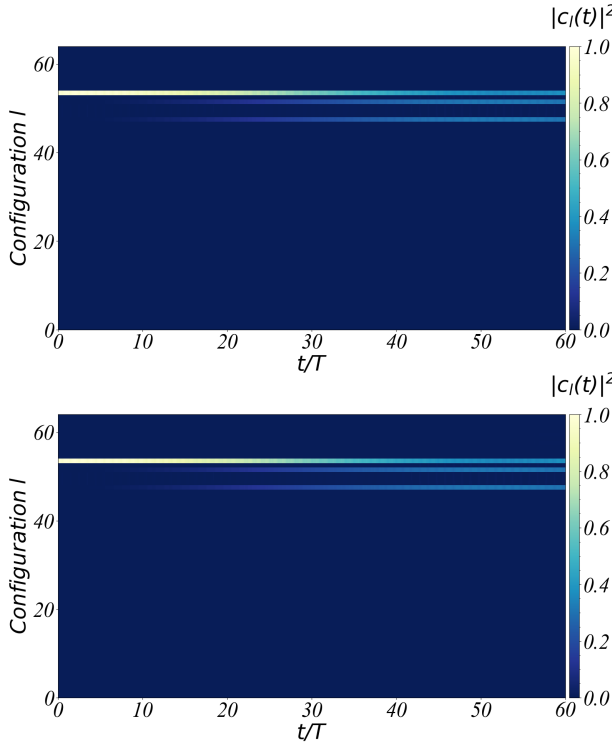


Figure 3. Populations associated to each configuration  $|c_l(t)|^2$  for the integer case  $\Omega = U/2$ , with  $T = 2\pi/\Omega$ , and a lattice with  $L = 3$  sites. The upper panel shows the system dynamics considering a closed scenario, whereas the lower panel an open scenario. In this simulation, we have considered all possible configurations in the Hilbert space which contains  $\mathcal{M} = 64$  configurations.

$|\psi(t)\rangle = \sum_{l=1}^{\mathcal{M}} c_l(t) |l\rangle$ , with  $\mathcal{M} = \sum_{N=0}^L D_{N,L}$  for fixed number of sites  $L$ . Therefore, it is necessary to compute the probability of all accessible configurations the system may visit along its dynamical evolution. In the three-site Bose-Hubbard lattice, there are  $\mathcal{M} = \sum_{N=0}^3 D_{N,3} = 64$  accessible configurations. The figure 3 shows the distribution of populations of each configuration  $|c_l(t)|^2$  for the fractional case  $\Omega = U/2$ . The upper panel shows the system dynamics considering a closed system, whereas the lower panel an open system scenario. In both cases, we see that the system populate the same configurations. We stress that, in the open system scenario, the probability to access states different from  $|\psi_0\rangle$  and  $|\psi_3\rangle$  is less than or equal to  $10^{-2}$ .

### B. The four-site Bose-Hubbard lattice

Let us consider the four site Bose-Hubbard lattice initialized in the state  $|\psi_0\rangle = |1111\rangle$ . In this case, there are  $\mathcal{M} = \sum_{N=0}^4 D_{N,4} = 625$  accessible configurations. As in the three-site Bose-Hubbard lattice, in figure 4 we plot the distribution of populations of each configuration  $|c_l(t)|^2$  for the fractional case  $\Omega = U/2$ . The upper panel shows the system dynamics considering a closed system, whereas the lower panel an open system scenario. In both cases, we see that

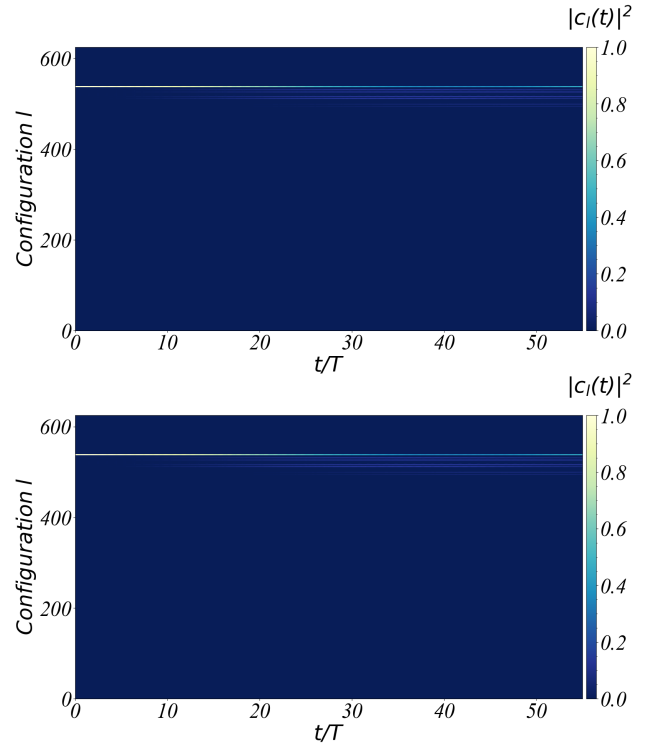


Figure 4. Populations associated to each configuration  $|c_l(t)|^2$  for the integer case  $\Omega = U/2$ , with  $T = 2\pi/\Omega$ , and a lattice with  $L = 4$  sites. The upper panel shows the system dynamics considering a closed scenario, whereas the lower panel an open scenario. In this simulation, we have considered all possible configurations in the Hilbert space which contains  $\mathcal{M} = 625$  configurations.

the system populate the same configurations. Therefore, we conclude that, for finite lattice sites, the slowing down characteristic of the fractional resonance is a stable phenomenon under noisy dynamics.

### C. The linear entropy

Another way to characterize the stability of the system under noisy mechanisms is using the linear entropy defined as  $S(\hat{\rho}) = 1 - \text{tr}(\hat{\rho}^2)$ , where  $\hat{\rho}$  is the system density matrix. In a closed system scenario, the linear entropy  $S(\hat{\rho}) = 0$  at all times since  $\hat{\rho}$  is a pure state. However, a realistic situation will necessarily imply the density matrix to be a statistical mixture. In the previous section, we demonstrated that the fractional many-body resonance and its characteristic slowing down of the dynamics [38] is a stable phenomenon under loss mechanisms. The latter is also reflected in linear entropy as shown in figure 5, where the upper (lower) panel shows the linear entropy as a function of time for a lattice of  $L = 3$  ( $L = 4$ ) sites. In both cases,  $S(\hat{\rho})$  is on the order of  $10^{-2}$  at the final evolution time.

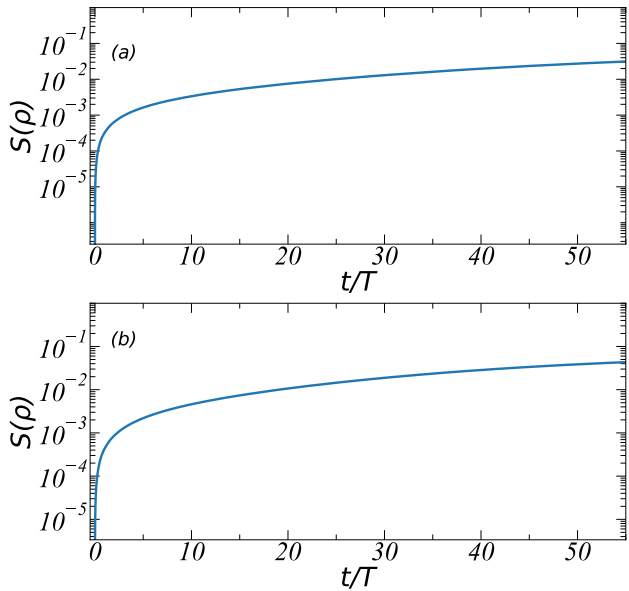


Figure 5. Panels (a,b) show the linear entropy as a function of time for fractional resonance condition  $\Omega = U/2$ , with  $T = 2\pi/\Omega$ , considering three and four site Bose Hubbard lattice, respectively.

#### IV. CONCLUSIONS

Considering small lattices of strongly interacting bosonic particles, we have provided robust evidence about the stability

of many-body resonances and its characteristic slowing down, under realistic parameters of NISQ devices implemented in superconducting circuits. Our investigation includes decay and dephasing mechanisms acting locally on each bosonic particle using the Lindblad master equation, which have been proven useful for describing state-of-the-art superconducting circuit experiments. In the short-term, we expect to extend our study to larger lattice sizes  $L > 10$  using the adaptive time-dependent density matrix renormalization group approach to further confirm the findings presented here. Our findings represent an important step before seeking potential applications of fractional resonances and their associated prethermal states as quantum memory device.

#### ACKNOWLEDGMENTS

We thank R. Román-Ancheyta for helpful discussions and carefully reading our article. R.P. acknowledges the support from Vicerrectoría de Postgrado USACH. G.R. acknowledges the support from Fondo Nacional de Desarrollo Científico y Tecnológico (FONDECYT, Chile) Grant No. 1190727.

---

[1] E. Altman, K. R. Brown, G. Carleo, L. D. Carr, E. Demler, C. Chin, B. DeMarco, S. E. Economou, M. A. Eriksson, K.-M. C. Fu, M. Greiner, K. R. Hazzard, R. G. Hulet, A. J. Kollár, B. L. Lev, M. D. Lukin, R. Ma, X. Mi, S. Misra, C. Monroe, K. Murch, Z. Nazario, K.-K. Ni, A. C. Potter, P. Roushan, M. Saffman, M. Schleier-Smith, I. Siddiqi, R. Simmonds, M. Singh, I. Spielman, K. Temme, D. S. Weiss, J. Vučković, V. Vuletić, J. Ye, and M. Zwierlein, “Quantum simulators: Architectures and opportunities,” *PRX Quantum* **2**, 017003 (2021).

[2] I. Bloch, J. Dalibard, and W. Zwerger, “Many-body physics with ultracold gases,” *Rev. Mod. Phys.* **80**, 885 (2008).

[3] M. Cheneau, P. Barmettler, D. Poletti, M. Endres, P. Schauß, T. Fukuhara, C. Gross, I. Bloch, C. Kollath, and S. Kuhr, “Light-cone-like spreading of correlations in a quantum many-body system,” *Nature* **481**, 484 (2012).

[4] H. Bernien, S. Schwartz, A. Keesling, H. Levine, A. Omran, H. Pichler, S. Choi, A. S. Zibrov, M. Endres, M. Greiner, V. Vuletić, and M. D. Lukin, “Probing many-body dynamics on a 51-atom quantum simulator,” *Nature* **551**, 579 (2017).

[5] J.-Y. Choi, S. Hild, J. Zeiher, P. Schauß, A. Rubio-Abadal, T. Yefsah, V. Khemani, D. A. Huse, I. Bloch, and C. Gross, “Exploring the many-body localization transition in two dimensions,” *Science* **352**, 1547 (2016).

[6] P. Roushan, C. Neill, J. Tangpanitanon, V. M. Bastidas, A. Megrant, R. Barends, Y. Chen, Z. Chen, B. Chiaro, A. Dunsworth, A. Fowler, B. Foxen, M. Giustina, E. Jeffrey, J. Kelly, E. Lucero, J. Mutus, M. Neeley, C. Quintana, D. Sank, A. Vainsencher, J. Wenner, T. White, H. Neven, D. G. Angelakis, and J. Martinis, “Spectroscopic signatures of localization with interacting photons in superconducting qubits,” *Science* **358**, 1175 (2017).

[7] R. Ma, B. Saxberg, C. Owens, N. Leung, Y. Lu, J. Simon, and D. I. Schuster, “A dissipatively stabilized mott insulator of photons,” *Nature* **566**, 51 (2019).

[8] Y. Ye, Z.-Y. Ge, Y. Wu, S. Wang, M. Gong, Y.-R. Zhang, Q. Zhu, R. Yang, S. Li, F. Liang, J. Lin, Y. Xu, C. Guo, L. Sun, C. Cheng, N. Ma, Z. Y. Meng, H. Deng, H. Rong, C.-Y. Lu, C.-Z. Peng, H. Fan, X. Zhu, and J.-W. Pan, “Propagation and localization of collective excitations on a 24-qubit superconducting processor,” *Phys. Rev. Lett.* **123**, 050502 (2019).

[9] C. Zha, V. M. Bastidas, M. Gong, Y. Wu, H. Rong, R. Yang, Y. Ye, S. Li, Q. Zhu, S. Wang, Y. Zhao, F. Liang, J. Lin, Y. Xu, C.-Z. Peng, J. Schmiedmayer, K. Nemoto, H. Deng, W. J. Munro, X. Zhu, and J.-W. Pan, “Ergodic-localized junctions in a periodically driven spin chain,” *Phys. Rev. Lett.* **125**, 170503 (2020).

[10] M. Gong, G. D. de Moraes Neto, C. Zha, Y. Wu, H. Rong, Y. Ye, S. Li, Q. Zhu, S. Wang, Y. Zhao, F. Liang, J. Lin, Y. Xu, C.-Z. Peng, H. Deng, A. Bayat, X. Zhu, and J.-W. Pan, “Experimental characterization of the quantum many-body localization transition,” *Phys. Rev. Research* **3**, 033043 (2021).

[11] C. Neill, P. Roushan, K. Kechedzhi, S. Boixo, S. V. Isakov, V. Smelyanskiy, A. Megrant, B. Chiaro, A. Dunsworth, K. Arya, R. Barends, B. Burkett, Y. Chen, Z. Chen, A. Fowler, B. Foxen, M. Giustina, R. Graff, E. Jeffrey, T. Huang, J. Kelly,

P. Klimov, E. Lucero, J. Mutus, M. Neeley, C. Quintana, D. Sank, A. Vainsencher, J. Wenner, T. C. White, H. Neven, and J. M. Martinis, “A blueprint for demonstrating quantum supremacy with superconducting qubits,” *Science* **360**, 195 (2018).

[12] K. Sacha, “Modeling spontaneous breaking of time-translation symmetry,” *Phys. Rev. A* **91**, 033617 (2015).

[13] D. V. Else, B. Bauer, and C. Nayak, “Floquet time crystals,” *Phys. Rev. Lett.* **117**, 090402 (2016).

[14] N. Y. Yao, A. C. Potter, I.-D. Potirniche, and A. Vishwanath, “Discrete time crystals: Rigidity, criticality, and realizations,” *Phys. Rev. Lett.* **118**, 030401 (2017).

[15] K. Sacha and J. Zakrzewski, “Time crystals: a review,” *Reports on Progress in Physics* **81**, 016401 (2017).

[16] A. Pizzi, J. Knolle, and A. Nunnenkamp, “Period- $n$  discrete time crystals and quasicrystals with ultracold bosons,” *Phys. Rev. Lett.* **123**, 150601 (2019).

[17] K. Sacha, *Time Crystals*, 1st ed., Springer Series on Atomic, Optical, and Plasma Physics, Vol. 114 (Springer, Cham, 2020).

[18] A. Pizzi, J. Knolle, and A. Nunnenkamp, “Higher-order and fractional discrete time crystals in clean long-range interacting systems,” *Nature Communications* **12**, 2341 (2021).

[19] A. Pizzi, A. Nunnenkamp, and J. Knolle, “Classical prethermal phases of matter,” *Phys. Rev. Lett.* **127**, 140602 (2021).

[20] A. Pizzi, A. Nunnenkamp, and J. Knolle, “Classical approaches to prethermal discrete time crystals in one, two, and three dimensions,” *Phys. Rev. B* **104**, 094308 (2021).

[21] H. P. Ojeda Collado, G. Usaj, C. A. Balseiro, D. H. Zanette, and J. Lorenzana, “Emergent parametric resonances and time-crystal phases in driven bardeen-cooper-schrieffer systems,” *Phys. Rev. Research* **3**, L042023 (2021).

[22] D. A. Abanin, W. De Roeck, and F. m. c. Huvveneers, “Exponentially slow heating in periodically driven many-body systems,” *Phys. Rev. Lett.* **115**, 256803 (2015).

[23] D. A. Abanin, W. De Roeck, W. W. Ho, and F. m. c. Huvveneers, “Effective hamiltonians, prethermalization, and slow energy absorption in periodically driven many-body systems,” *Phys. Rev. B* **95**, 014112 (2017).

[24] D. Abanin, W. De Roeck, W. W. Ho, and F. Huvveneers, “A rigorous theory of many-body prethermalization for periodically driven and closed quantum systems,” *Communications in Mathematical Physics* **354**, 809 (2017).

[25] T. Mori, T. Kuwahara, and K. Saito, “Rigorous bound on energy absorption and generic relaxation in periodically driven quantum systems,” *Phys. Rev. Lett.* **116**, 120401 (2016).

[26] T. Kuwahara, T. Mori, and K. Saito, “Floquet–magnus theory and generic transient dynamics in periodically driven many-body quantum systems,” *Annals of Physics* **367**, 96 (2016).

[27] A. Rubio-Abadal, M. Ippoliti, S. Hollerith, D. Wei, J. Rui, S. L. Sondhi, V. Khemani, C. Gross, and I. Bloch, “Floquet prethermalization in a bose-hubbard system,” *Phys. Rev. X* **10**, 021044 (2020).

[28] C. Ying, Q. Guo, S. Li, M. Gong, X.-H. Deng, F. Chen, C. Zha, Y. Ye, C. Wang, Q. Zhu, S. Wang, Y. Zhao, H. Qian, S. Guo, Y. Wu, H. Rong, H. Deng, F. Liang, J. Lin, Y. Xu, C.-Z. Peng, C.-Y. Lu, Z.-Q. Yin, X. Zhu, and J.-W. Pan, “Floquet prethermal phase protected by  $u(1)$  symmetry on a superconducting quantum processor,” *Phys. Rev. A* **105**, 012418 (2022).

[29] E. G. D. Torre and D. Dentelski, “Statistical Floquet prethermalization of the Bose-Hubbard model,” *SciPost Phys.* **11**, 40 (2021).

[30] J. Dziarmaga, “Dynamics of a quantum phase transition and relaxation to a steady state,” *Advances in Physics* **59**, 1063 (2010).

[31] A. Polkovnikov, K. Sengupta, A. Silva, and M. Vengalattore, “Colloquium: Nonequilibrium dynamics of closed interacting quantum systems,” *Rev. Mod. Phys.* **83**, 863 (2011).

[32] J. Eisert, M. Friesdorf, and C. Gogolin, “Quantum many-body systems out of equilibrium,” *Nature Physics* **11**, 124 (2015).

[33] A. Mitra, “Quantum quench dynamics,” *Annual Review of Condensed Matter Physics* **9**, 245 (2018).

[34] M. Heyl, “Dynamical quantum phase transitions: a review,” *Reports on Progress in Physics* **81**, 054001 (2018).

[35] R. Orús, “Tensor networks for complex quantum systems,” *Nature Reviews Physics* **1**, 538 (2019).

[36] U. Schollwöck, “The density-matrix renormalization group in the age of matrix product states,” *Annals of Physics* **326**, 96 (2011).

[37] P. Silvi, F. Tschirsich, M. Gerster, J. Jünemann, D. Jaschke, M. Rizzi, and S. Montangero, “The Tensor Networks Anthology: Simulation techniques for many-body quantum lattice systems,” *SciPost Phys. Lect. Notes* **8** (2019).

[38] R. Peña, V. M. Bastidas, F. Torres, W. J. Munro, and G. Romero, “Fractional resonances and prethermal states in floquet systems,” *Phys. Rev. B* **106**, 064307 (2022).

[39] M. P. A. Fisher, P. B. Weichman, G. Grinstein, and D. S. Fisher, “Boson localization and the superfluid-insulator transition,” *Phys. Rev. B* **40**, 546 (1989).

[40] D. Jaksch, C. Bruder, J. I. Cirac, C. W. Gardiner, and P. Zoller, “Cold bosonic atoms in optical lattices,” *Phys. Rev. Lett.* **81**, 3108 (1998).

[41] W. Chen, K. Hida, and B. C. Sanctuary, “Ground-state phase diagram of  $s = 1$  XXZ chains with uniaxial single-ion-type anisotropy,” *Phys. Rev. B* **67**, 104401 (2003).

[42] W. C. Chung, J. de Hond, J. Xiang, E. Cruz-Colón, and W. Ketterle, “Tunable single-ion anisotropy in spin-1 models realized with ultracold atoms,” *Phys. Rev. Lett.* **126**, 163203 (2021).

[43] A. D. Greentree, C. Tahan, J. H. Cole, and L. C. L. Hollenberg, “Quantum phase transitions of light,” *Nat Phys* **2**, 856 (2006).

[44] M. J. Hartmann, F. G. S. L. Brandao, and M. B. Plenio, “Strongly interacting polaritons in coupled arrays of cavities,” *Nat Phys* **2**, 849 (2006).

[45] D. G. Angelakis, M. F. Santos, and S. Bose, “Photon-blockade-induced mott transitions and  $xy$  spin models in coupled cavity arrays,” *Phys. Rev. A* **76**, 031805 (2007).

[46] E. van Nieuwenburg, Y. Baum, and G. Refael, “From bloch oscillations to many-body localization in clean interacting systems,” *Proceedings of the National Academy of Sciences* **116**, 9269 (2019), <https://www.pnas.org/doi/pdf/10.1073/pnas.1819316116>.

[47] U. Mishra and A. Bayat, “Driving enhanced quantum sensing in partially accessible many-body systems,” *Phys. Rev. Lett.* **127**, 080504 (2021).

[48] M. A. Nielsen and I. L. Chuang, *Quantum Computation and Quantum Information* (Cambridge University Press, 2000).

[49] P. Wittek, *Quantum Machine Learning : What Quantum Computing Means to Data Mining* (Academic Press, 2014) p. 176.

[50] G. Carleo, I. Cirac, K. Cranmer, L. Daudet, M. Schuld, N. Tishby, L. Vogt-Maranto, and L. Zdeborová, “Machine learning and the physical sciences,” *Rev. Mod. Phys.* **91**, 045002 (2019).

[51] M. Schuld and F. Petruccione, *Machine Learning with Quantum Computers*, Quantum Science and Technology (Springer International Publishing, 2021).

[52] P. Shor, in *Proceedings 35th Annual Symposium on Foundations of Computer Science* (1994) pp. 124–134.

[53] A. Aspuru-Guzik, A. D. Dutoi, P. J. Love, and M. Head-Gordon, “Simulated Quantum Computation of Molecular En-

ergies,” *Science* **309**, 1704 (2005).

[54] I. M. Georgescu, S. Ashhab, and F. Nori, “Quantum simulation,” *Rev. Mod. Phys.* **86**, 153 (2014).

[55] Y. Cao, J. Romero, J. P. Olson, M. Degroote, P. D. Johnson, M. Kieferová, I. D. Kivlichan, T. Menke, B. Peropadre, N. P. D. Sawaya, *et al.*, “Quantum Chemistry in the Age of Quantum Computing,” *Chem. Rev.* **119**, 10856 (2019).

[56] S. McArdle, S. Endo, A. Aspuru-Guzik, S. C. Benjamin, and X. Yuan, “Quantum computational chemistry,” *Rev. Mod. Phys.* **92**, 015003 (2020).

[57] J. Preskill, “Quantum Computing in the NISQ era and beyond,” *Quantum* **2**, 79 (2018), 1801.00862v3.

[58] F. Arute, K. Arya, R. Babbush, D. Bacon, J. C. Bardin, R. Barends, R. Biswas, S. Boixo, F. G. S. L. Brandao, D. A. Buell, *et al.*, “Quantum supremacy using a programmable superconducting processor,” *Nature* **574**, 505 (2019).

[59] H.-S. Zhong, H. Wang, Y.-H. Deng, M.-C. Chen, L.-C. Peng, Y.-H. Luo, J. Qin, D. Wu, X. Ding, Y. Hu, *et al.*, “Quantum computational advantage using photons,” *Science* **370**, 1460 (2020).

[60] Y. Wu, W.-S. Bao, S. Cao, F. Chen, M.-C. Chen, X. Chen, T.-H. Chung, H. Deng, Y. Du, D. Fan, *et al.*, “Strong Quantum Computational Advantage Using a Superconducting Quantum Processor,” *Phys. Rev. Lett.* **127**, 180501 (2021).

[61] L. S. Madsen, F. Laudenbach, M. Falamarzi. Askarani, F. Rortais, T. Vincent, J. F. F. Bulmer, F. M. Miatto, L. Neuhaus, L. G. Helt, M. J. Collins, *et al.*, “Quantum computational advantage with a programmable photonic processor,” *Nature* **606**, 75 (2022).

[62] K. Bharti, A. Cervera-Lierta, T. H. Kyaw, T. Haug, S. Alperin-Lea, A. Anand, M. Degroote, H. Heimonen, J. S. Kottmann, T. Menke, *et al.*, “Noisy intermediate-scale quantum algorithms,” *Rev. Mod. Phys.* **94**, 015004 (2022).

[63] S. Chen, J. Cotler, H.-Y. Huang, and J. Li, “Exponential separations between learning with and without quantum memory,” *arXiv2111.05881* (2021).

[64] H.-Y. Huang, M. Broughton, J. Cotler, S. Chen, J. Li, M. Mohseni, H. Neven, R. Babbush, R. Kueng, J. Preskill, *et al.*, “Quantum advantage in learning from experiments,” *arXiv2112.00778* (2021).

[65] D. Aharonov, J. Cotler, and X.-L. Qi, “Quantum algorithmic measurement,” *Nat. Commun.* **13**, 1 (2022).

[66] A. W. Harrow, A. Hassidim, and S. Lloyd, “Quantum Algorithm for Linear Systems of Equations,” *Phys. Rev. Lett.* **103**, 150502 (2009).

[67] S. Lloyd, M. Mohseni, and P. Rebentrost, “Quantum principal component analysis,” *Nat. Phys.* **10**, 631 (2014).

[68] V. Giovannetti, S. Lloyd, and L. Maccone, “Quantum Random Access Memory,” *Phys. Rev. Lett.* **100**, 160501 (2008).

[69] T. H. Kyaw, S. Felicetti, G. Romero, E. Solano, and L.-C. Kwek, “Scalable quantum memory in the ultrastrong coupling regime,” *Sci. Rep.* **5**, 1 (2015).

[70] R. Nandkishore and D. A. Huse, “Many-body localization and thermalization in quantum statistical mechanics,” *Annual Review of Condensed Matter Physics* **6**, 15 (2015), <https://doi.org/10.1146/annurev-conmatphys-031214-014726>.

[71] D. A. Abanin, E. Altman, I. Bloch, and M. Serbyn, “Colloquium: Many-body localization, thermalization, and entanglement,” *Rev. Mod. Phys.* **91**, 021001 (2019).

[72] F. Alet and N. Laflorencie, “Many-body localization: An introduction and selected topics,” *Comptes Rendus Physique* **19**, 498 (2018), quantum simulation / Simulation quantique.

[73] A. Nico-Katz, A. Bayat, and S. Bose, “Information-theoretic memory scaling in the many-body localization transition,” *Phys. Rev. B* **105**, 205133 (2022).

[74] B. V. Chirikov, “A universal instability of many-dimensional oscillator systems,” *Physics Reports* **52**, 263 (1979).

[75] R. Moessner and S. L. Sondhi, “Equilibration and order in quantum floquet matter,” *Nature Physics* **13**, 424 (2017).

[76] M. Bukov, L. D’Alessio, and A. Polkovnikov, “Universal high-frequency behavior of periodically driven systems: from dynamical stabilization to floquet engineering,” *Advances in Physics* **64**, 139 (2015).

[77] S. Blanes, F. Casas, J. A. Oteo, and J. Ros, “A pedagogical approach to the magnus expansion,” *European Journal of Physics* **31**, 907 (2010).

[78] M. P. A. Fisher, P. B. Weichman, G. Grinstein, and D. S. Fisher, “Boson localization and the superfluid-insulator transition,” *Phys. Rev. B* **40**, 546 (1989).

[79] T. D. Kühner, S. R. White, and H. Monien, “One-dimensional bose-hubbard model with nearest-neighbor interaction,” *Phys. Rev. B* **61**, 12474 (2000).

[80] J. Raftery, D. Sadri, S. Schmidt, H. E. Türeci, and A. A. Houck, “Observation of a dissipation-induced classical to quantum transition,” *Phys. Rev. X* **4**, 031043 (2014).

[81] D. L. Underwood, W. E. Shanks, A. C. Y. Li, L. Ateshian, J. Koch, and A. A. Houck, “Imaging photon lattice states by scanning defect microscopy,” *Phys. Rev. X* **6**, 021044 (2016).

[82] M. Fitzpatrick, N. M. Sundaresan, A. C. Y. Li, J. Koch, and A. A. Houck, “Observation of a dissipative phase transition in a one-dimensional circuit qed lattice,” *Phys. Rev. X* **7**, 011016 (2017).

[83] M. J. Peterer, S. J. Bader, X. Jin, F. Yan, A. Kamal, T. J. Gudmundsen, P. J. Leek, T. P. Orlando, W. D. Oliver, and S. Gustavsson, “Coherence and decay of higher energy levels of a superconducting transmon qubit,” *Phys. Rev. Lett.* **114**, 010501 (2015).